TECHNICAL ARTICLE

Mechanism and kinetics of early transition metal hydrides, oxides, and chlorides to enhance hydrogen release and uptake properties of MgH_2

Dmytro Korablov,[1] Thomas K. Nielsen,[1] Flemming Besenbacher,[2] and Torben R. Jensen[1,a)]
[1]*Department of Chemistry, Center for Materials Crystallography (CMC), Interdisciplinary Nanoscience Center (iNANO), Aarhus University, Langelandsgade 140, DK-8000 Aarhus C, Denmark*
[2]*Interdisciplinary Nanoscience Center (iNANO) and Department of Physics and Astronomy, Aarhus University, Ny Munkegade 120, DK-8000 Aarhus C, Denmark*

(Received 30 September 2014; accepted 5 January 2015)

Selected hydrides (TiH_2, ZrH_2), chlorides (VCl_3, $ScCl_3$) or oxides (V_2O_5) utilized as additives facilitating hydrogen release and uptake for magnesium hydride were investigated using mechano-chemical treatment and *in-situ* synchrotron radiation powder X-ray diffraction studies. The fastest hydrogen desorption and absorption kinetics for MgH_2 was observed for a sample with 5 mol% V_2O_5 at 320 °C. Additional activation of the system (2 cycles, vacuum/$p(H_2)$ ~150 bar, 450 °C) leads to significant improvement of the kinetics even at lower temperatures, 270 °C. The observed prolific effect is achieved through the full reduction of vanadium oxides and formation of an efficient vanadium catalyst as nanoparticles and possibly interfacial effects in the MgO/Mg/MgH_2/V system introduced during cycling hydrogen release and uptake in hydrogen/dynamic vacuum at 450 °C. Nanostructuring as well as hydrogen permeability via vanadium nanoparticles may improve kinetics and reduce the apparent activation energy for hydrogen release. Thus, the enhancement of hydrogen release/uptake in the MgH_2 owe to "*in situ*" formation of vanadium nanoparticles by reduction of V_2O_5. © *2015 International Centre for Diffraction Data*. [doi:10.1017/S0885715615000056]

Key words: hydrogen storage, magnesium hydride, vanadium pentoxide, ball milling, *in situ* synchrotron powder X-ray diffraction

I. INTRODUCTION

Currently, magnesium hydride is the subject of many scientific studies as a promising material for hydrogen storage. Obstacles to its widespread use are the high decomposition temperature (~300 °C) and the slow kinetics of hydrogen absorption–desorption. Traditionally, the solution to these problems is found in nanostructuring that can be achieved, for example, by mechano-chemical treatment (Huot *et al.*, 1999; Paskevicius *et al.*, 2010), use of effective catalysts (Schimmel *et al.*, 2005; Varin *et al.*, 2011) or by introducing of additives that alter the thermodynamic properties of the system (Jin *et al.*, 2007a; Cuevas *et al.*, 2012). Nanosized metals may have lower melting point or spontaneous alloying as compared with their bulk form (Hirokazu and Kitagawa, 2012). In addition, nanostructuring by mechano-chemical treatment often improve kinetics but may also lead to surface contamination with material from the milling equipment (Pasquini *et al.*, 2011; Huot *et al.*, 2013). A remaining challenge is the stabilization of magnesium nanoparticles and preventing agglomeration, sintering, oxidation, and potential side reactions leading to rapid deterioration of material properties upon cycling (Sato and Ishikawa, 2012). Nanoconfinement of magnesium has been investigated and was shown to increase the kinetics for hydrogen release and uptake and may also provide improved thermodynamic properties (Nielsen *et al.*, 2009, 2011; Paskevicius *et al.*, 2010; Vajo, 2011).

A wide range of different types of additives including metals, oxides, halides, and hydrides has been considered for possible prolific effects on hydrogen release and uptake. Nanonickel (n-Ni) is well established as efficient catalyst for the Mg/MgH_2 system, which acts via the intermediate Mg_2NiH_4 (Jensen *et al.*, 2006; Varin *et al.*, 2009, 2011; Pasquini *et al.*, 2011; Callini *et al.*, 2013). Other metals, e.g., Al, Ti, Cu, Pd may have both a thermodynamic and kinetic effect by forming magnesium containing alloys (Andreasen *et al.*, 2005, 2006; Callini *et al.*, 2010). In particular, titanium is relevant because of low costs, lighter weight, and fast kinetics for hydrogen release and uptake for Mg/MgH_2. Moreover, magnesium does not form intermetallic compounds with V and Nb (Massalski, 1990). Therefore, both metals are considered as heterogeneous catalysts (Schimmel *et al.*, 2005).

Transition metal oxides are also good catalysts for enhancement of hydrogen release and uptake e.g., Nb_2O_5 (Barkhordarian *et al.*, 2006) and V_2O_5 (Oelerich *et al.*, 2001a, 2001b; Jung *et al.*, 2006). A drawback may be that some metal oxides have a tendency to reduce during cycling hydrogen release and uptake, which leads to the formation of inert magnesium oxide. The detailed mechanism for metal oxides prolific action may be complex and in some cases is not fully understood. An *in situ* synchrotron radiation powder X-ray diffraction (SR-PXD) investigation of MgH_2 and Nb_2O_5 (8 mol%) revealed reduction of Nb(V) and

a)Author to whom correspondence should be addressed. Electronic mail: trj@chem.au.dk

formation of $Mg_{1-x}Nb_xO$, which may facilitate release and uptake of hydrogen (Nielsen and Jensen, 2012).

Transition metal halides have also been successfully utilized as additives for improving the kinetics of the absorption/desorption of hydrogen in MgH_2, e.g., VCl_3 and $TiCl_3$ (Malka *et al.*, 2010). Moreover, halides of Fe, Ni, and Nb have also shown attractive catalytic properties (Ivanov *et al.*, 2003; Deledda *et al.*, 2005; Bhat *et al.*, 2006; Kim *et al.*, 2008; Ma *et al.*, 2009).

Transition metal oxides and halides may in some cases react with MgH_2 or Mg and form other compounds. Currently, there is no clear picture of their mechanism of action and the active compound may not be known (Barkhordarian *et al.*, 2006; Jin *et al.*, 2007b). This has prompted the present investigation of binary early *d*-block hydrides, oxides, and chlorides used as additives for the Mg/MgH_2 system. We utilize *in situ* SR-PXD to provide a more detailed picture of mechanism for hydrogen release and uptake as well as identification of active compounds in the mixtures.

II. EXPERIMENTAL

A. Sample preparation

Mixtures of MgH_2 (98%, Alfa Aesar) with 5 mol% of additive were ball milled under argon atmosphere using tungsten carbide (WC) hard alloy vial (80 ml) and balls (10 mm diameter) in a Fritsch Pulverisette P4 planetary mill. As additives, commercially available chemicals were used: vanadium pentoxide (V_2O_5, 98 + %, Aldrich), titanium hydride (TiH_2, 98%, Aldrich), zirconium hydride (ZrH_2, 99%, Aldrich), vanadium chloride (VCl_3, 97%, Aldrich), and scandium chloride ($ScCl_3$, 99.9%, Aldrich). The typical mass of each mixture constituted 3 g with 1 : 41 powder-to-ball weight ratio. The milling was performed in time intervals of 30 min at a rotation speed of 300 rpm (Huot *et al.*, 2013).

Experimental details regarding samples composition and preparation can be found in Table I. All handling and manipulation of the chemicals were carried out under argon atmosphere in an MBraun Unilab glove box with a recirculation gas purification system and gas/humidity sensors. Oxygen and water levels were kept well below 1 ppm during all operations.

B. *In situ* synchrotron radiation powder X-ray diffraction (SR-PXD)

The detailed reaction mechanisms and kinetics of hydrogen release and uptake in MgH_2 with different additives were studied by *in situ* SR-PXD experiments. Data were collected at beamline I711 at the synchrotron MAX II, in the research laboratory MAX-lab, Lund, Sweden using a Mar165 CCD detector. A LaB_6 external standard was used to determine sample-detector distance, detector orientation, and the wavelength. The samples were mounted in sapphire single crystal tubes (Al_2O_3, o.d. 1.09 mm, i.d. 0.79 mm) in an argon-filled glove box ($p(O_2, H_2O) < 1$ ppm). The sample holder was specially developed for the study of gas/solid reactions and hydrogen pressures were allowed up to 20 MPa and temperatures from room temperature (RT) to 800 °C (Jensen *et al.*, 2010). The selected wavelength was 0.94608 Å and the X-ray exposure time was 5 s per PXD pattern. Samples for investigation of mechanism and kinetics of hydrogen release and uptake were heated stepwise to fixed temperatures of 270 and 320 °C (15 °C min^{-1}) in a hydrogen pressure of 100–150 bar. The hydrogen pressure was reduced to $p(H_2)$ $\sim 10^{-2}$ bar (dynamic vacuum) when the fixed temperature was reached and then again increased to 100–150 bar when the sample was fully dehydrogenated (after 15 to 30 min) measuring one full hydrogen release and uptake cycle at each temperature. Selected samples were additionally heated to 450 °C and two extra H_2 desorption/absorption cycles were performed. Finally, the samples were cooled to 270 °C and one dehydrogenation was conducted.

All obtained raw images were transformed to two-dimensional powder patterns using the FIT2D program (Hammersley *et al.*, 1996), which was also used for calibration using measurements of the standard NIST LaB_6 sample. Crystal structure refinements were performed using the Rietveld method implemented in the Fullprof program (Rodríguez-Carvajal, 1993). The backgrounds were described by linear interpolation between selected points, while pseudo-Voigt profile functions were used to fit the diffraction peaks. Sequential refinements provide the weight fractions for the compounds present in the sample as a function of time. The extracted normalized curves represent phase formation or decomposition curves as a function of time denoted $\alpha(t)$. These sigmoidal shaped curves can be used for evaluation of the activation process.

The decomposition curves for MgH_2 can be fitted well with the equation of shrinking core model:

$$1 - (1 - \alpha)^{1/2} = kt \quad (1)$$

where α is the phase fraction at time t and k is the rate constant (Liang *et al.*, 2000; Varin *et al.*, 2009).

An apparent activation energy, E_A, and a pre-factor, A, for the overall reaction can be calculated using Arrhenius law:

$$k = A \exp(-E_A/RT) \quad (2)$$

where R is the gas constant and T is the absolute temperature.

TABLE I. Composition of the MgH_2 + additives samples prepared mechano-chemically.

Sample notation		Composition (mol%) MgH_2	additive	Ball milling conditions time (min) (interval, brake)	Ball to powder weight ratio	Rotation speed (rpm)
S1	$MgH_2 + V_2O_5$	95	5	30 (6*5, 3)	41 : 1	300
S2	$MgH_2 + ZrH_2$	95	5	30 (6*5, 3)	41 : 1	300
S3	$MgH_2 + TiH_2$	95	5	30 (6*5, 3)	41 : 1	300
S4	$MgH_2 + ScCl_3$	95	5	30 (6*5, 3)	41 : 1	300
S5	$MgH_2 + VCl_3$	95	5	30 (6*5, 3)	41 : 1	300

https://doi.org/10.1017/S0885715615000056 Published online by Cambridge University Press

III. RESULTS AND DISCUSSION

A. Reactions during mechano-chemical and heat treatment

Dispersion of transition metals in Mg/MgH_2 system is difficult because of the ductility of the metals. Therefore, binary salt-like oxides, chlorides, and hydrides based on early *d*-block metals were selected as additives in the present investigation, i.e., V_2O_5, VCl_3, $ScCl_3$, TiH_2, and ZrH_2.

Figures 1–5 show *in situ* SR-PXD data for the ball-milled samples S1–S5 (see Table I), respectively. Bragg diffraction peaks of β-, γ-MgH_2, and MgO are observed for sample S1 (Figure 1) at RT. There is no observed diffraction from V_2O_5, which suggests that a redox reaction has occurred during mechano-chemical treatment [see reaction scheme (3)]. Decomposition of MgH_2 initiates at 270 °C by decreasing excess hydrogen pressure below equilibrium at this temperature. All γ-MgH_2 disappears within <1 min of heating at 270 °C and most of the present β-MgH_2 (90%) is decomposed after 10 min (during measurement of 40 PXD patterns). The PXD data show the presence of Mg, MgO, and possibly V at 270 °C. The latter two phases are difficult to distinguish owing to overlapping Bragg reflections.

$$5MgH_2 + V_2O_5 \rightarrow 2\,V + 5MgO + 5H_2 \qquad (3)$$

PXD patterns of the samples S2 and S3 measured at RT reveal diffracted intensities from the reactants only, i.e., no reaction has occurred between ZrH_2 or TiH_2 and MgH_2. Notice that there is no observed diffraction from MgO in sample S2 and S3. This indicates that the presence of MgO in S1 is because of a reaction between V_2O_5 and MgH_2. Magnesium metal formation in both samples, S2 and S3, initiates at 270 °C when the pressure is reduced.

The as-milled chloride doped sample S4 reveals diffraction from MgH_2 and scandium(II) hydride ScH_2 and no diffraction from the additive, $ScCl_3$. This indicates that a redox reaction has occurred during ball-milling [see reaction scheme (4)]. Formation of magnesium initiates when the pressure is reduced at 270 °C. Formation of $MgCl_2$ is observed during the rehydrogenation at $p(H_2) = 100$ bar.

$$5MgH_2 + ScCl_3 \rightarrow MgCl_2 + ScH_2 + 0.5H_2 \qquad (4)$$

Sample S5 ($MgH_2 - VCl_3$) behaves in a similar way, i.e., no observation of VCl_3 after milling, crystallization of $MgCl_2$

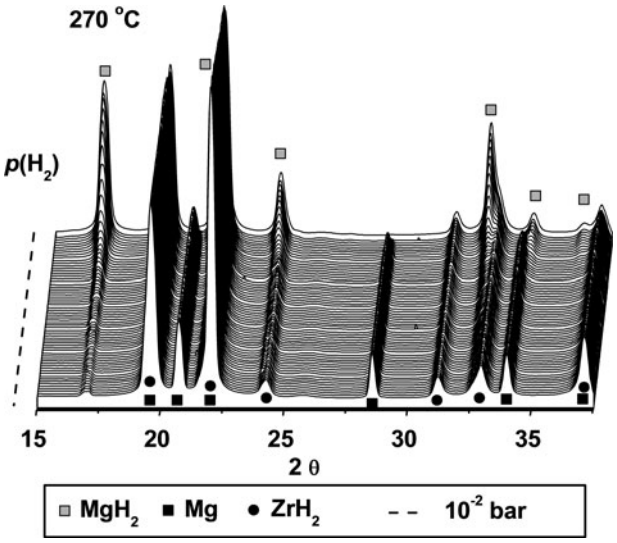

Figure 2. *In-situ* SR-PXD data measured for sample MgH_2–ZrH_2 (S2) heated under $p(H_2) = 100$ bar from RT to 270 °C (15 °C min^{-1}) and subsequently dehydrogenated at this temperature applying $p(H_2) = 10^{-2}$ (λ = 0.946 08 Å).

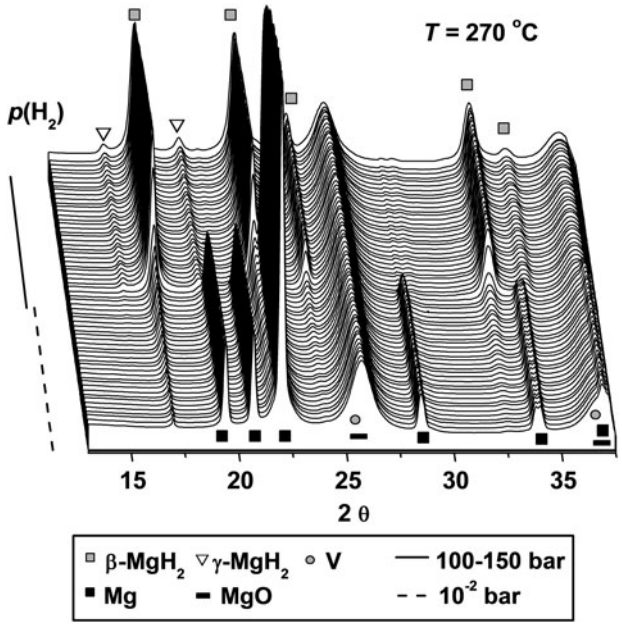

Figure 1. *In-situ* SR-PXD data measured for sample MgH_2–V_2O_5 (S1) heated under $p(H_2) = 100$ bar from RT to 270 °C (15 °C min^{-1}) and subsequently dehydrogenated and hydrogenated at this temperature applying alternately $p(H_2) = 10^{-2}$ and 100–150 bar (λ = 0.946 08 Å).

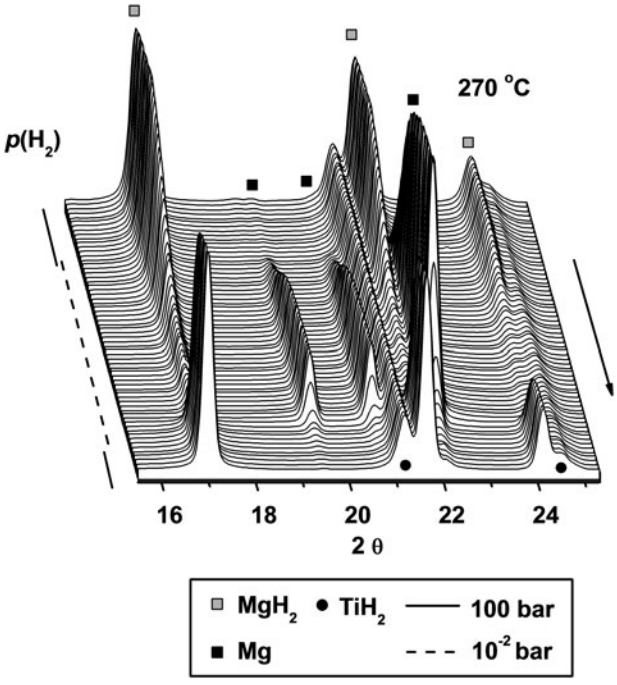

Figure 3. *In-situ* SR-PXD data measured for sample MgH_2–TiH_2 (S3) heated under $p(H_2) = 100$ bar from RT to 270 °C (15 °C min^{-1}) and subsequently cycled at this temperature applying alternately $p(H_2) = 10^{-2}$ and 100–150 bar (λ = 0.946 08 Å).

https://doi.org/10.1017/S0885715615000056 Published online by Cambridge University Press

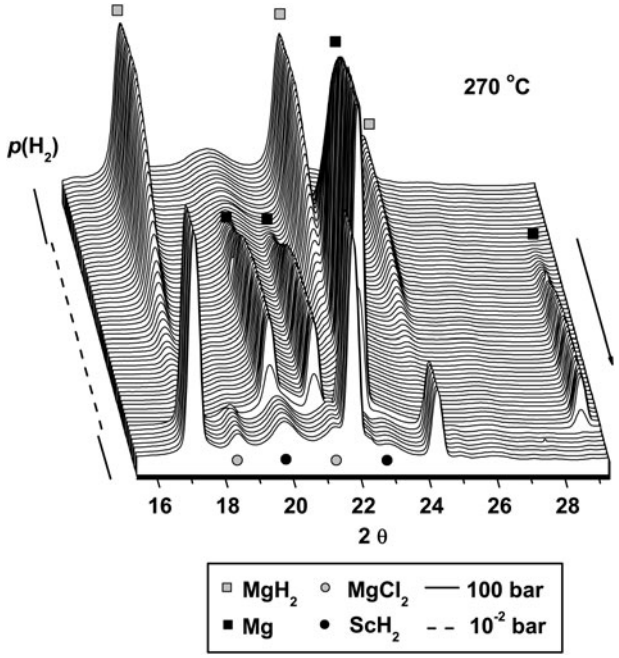

Figure 4. *In-situ* SR-PXD data measured for sample MgH_2–$ScCl_3$ (S4) heated under $p(H_2) = 100$ bar from RT to 270 °C (15 °C min^{-1}) and subsequently cycled at this temperature applying alternately $p(H_2) = 10^{-2}$ and 100–150 bar ($\lambda = 0.946\ 08$ Å).

during rehydrogenation (see Figure 5). Furthermore, unidentified reflection reveals a continuous change in composition at $2\theta = 24.9$–$25.4°$ under vacuum.

B. Evaluation of additives kinetic effect

In situ SR-PXD data are used to investigate the effect of selected early *d*-block hydrides, oxides, and chlorides additives on the mechanism of hydrogen release and uptake in magnesium hydride system at 270 °C. The diffracted intensities from MgH_2 are integrated, normalized, and converted to phase fraction and used to visualize decreasing amounts of MgH_2 during dehydrogenation reactions (Figure 6). At 270 °C the weakest kinetic effect for hydrogen desorption is provided by $ScCl_3$ (S4) and TiH_2 (S3) and the strongest influence is provided by VCl_3 (S5) and V_2O_5 (S1). In the early stages of MgH_2 decomposition V_2O_5 demonstrates the fastest kinetics, which is somewhat slowed down in the late stage of the decomposition. In contrast, the effect from VCl_3 additive is also significant in the late stage of the decomposition. Zirconium hydride (S2) has an intermediate kinetic effect. A similar analysis of additives effect was also performed at higher temperature of 320 °C and the results are presented in Figure 7. The time scale for these experiments is clearly shorter as compared with those performed at 270 °C. In addition, the additives ability to accelerate the reaction kinetics follows the sequence: $ScCl_3 < TiH_2 < ZrH_2 < VCl_3 < V_2O_5$. These experiments reveal that the effect of increasing temperatures on the acceleration of reaction rate is more pronounced

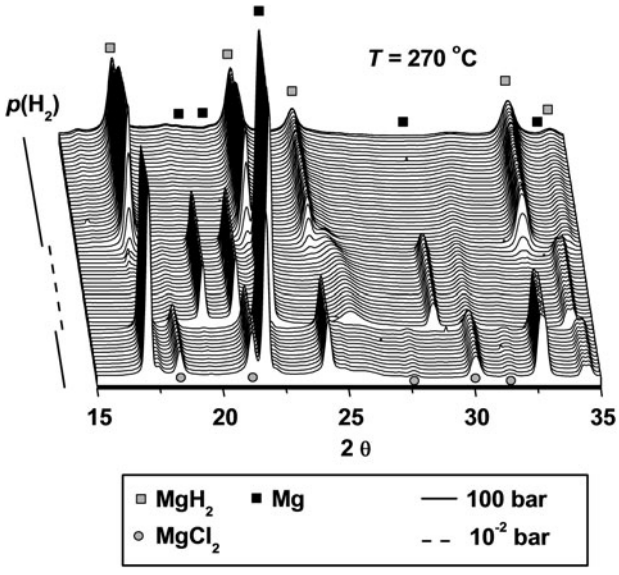

Figure 5. *In-situ* SR-PXD data measured for sample MgH_2-VCl_3 (S5) heated under $p(H_2) = 100$ bar from RT to 270 °C (15 °C min^{-1}) and subsequently cycled at this temperature applying alternately $p(H_2) = 10^{-2}$ and 100–150 bar ($\lambda = 0.946\ 08$ Å).

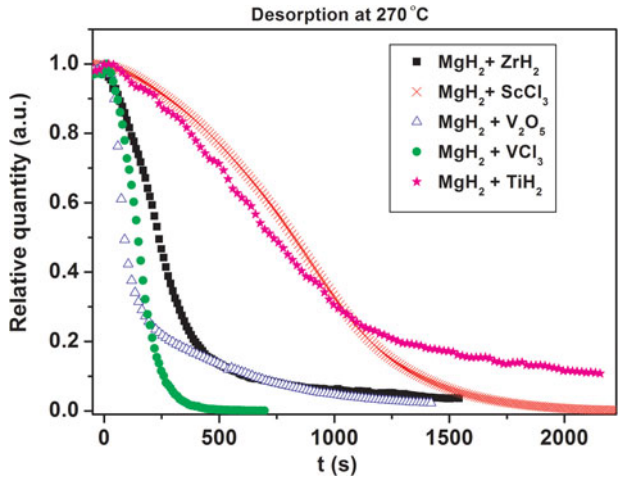

Figure 6. (color online) Integrated normalized diffracted intensities for samples S1–S5 showing changes in the relative amount of MgH_2 at 270 °C as a function of time.

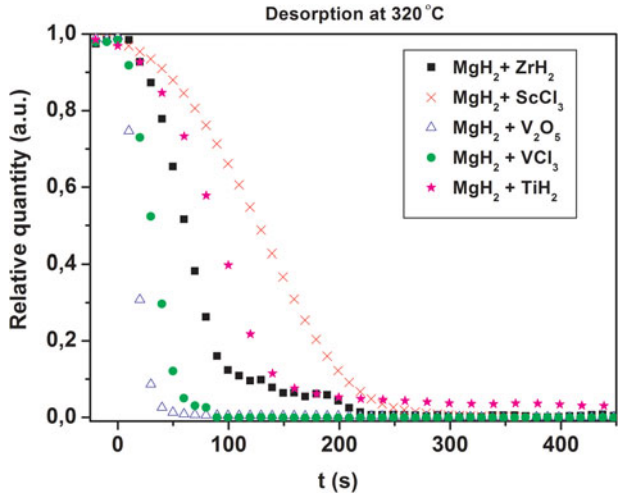

Figure 7. (color online) Integrated normalized diffracted intensities for samples S1–S5 showing changes in the relative amount of MgH_2 at 320 °C as a function of time.

https://doi.org/10.1017/S0885715615000056 Published online by Cambridge University Press

than the different additives effect. It should be emphasized that commercial MgH_2 ball-milled without additives in the same conditions does not desorb hydrogen at 270 nor at 320 °C. Slight yield of hydrogen begins to be observed only at temperatures above 350 °C.

C. Activation of magnesium hydride via a chemical reaction

Analysis of the additives effect (Section B) revealed that the best results were obtained using the addition of V_2O_5. Here we further analyse the mechanism for this effect. Bragg diffraction peaks of β-, γ-MgH_2 and MgO are observed for MgH_2–V_2O_5 (S1) (see Figure 1), at RT. There is no observed diffraction from V_2O_5, which suggest that a redox reaction has occurred during mechano-chemical treatment [see reaction scheme (3)]. To crystallize possible reaction products the same sample was heated to 450 °C and 2 cycles of hydrogen release and uptake were conducted (see Figure 8). Diffraction peaks from V_2H are clearly observed at $2\theta = 24.5°$ and 35.9° in the hydrogenated state when the temperature reaches 450 °C and for V in the dehydrogenated state at $2\theta = 25.4°$ and 36.4°. This leads to the splitting of the peak previously assigned to MgO and V, at $2\theta \approx 26°$ in Figure 1. Apparently, the heating procedure fully reduced the possibly remaining V_2O_5 and facilitated crystallization of V_2H/V. The experiment was continued using the same sample (see Figure 9), the temperature was decreased to 270 °C and one dehydrogenation was conducted similar to what is shown in Figure 1. Presence of vanadium and vanadium hydride is more clearly observed in Figure 9 as compared with Figure 8 and during dehydrogenation diffraction peaks from V_2H (at $2\theta = 24.4°$) continuously change position to $2\theta = 25.5°$ because of the release of hydrogen and formation of V.

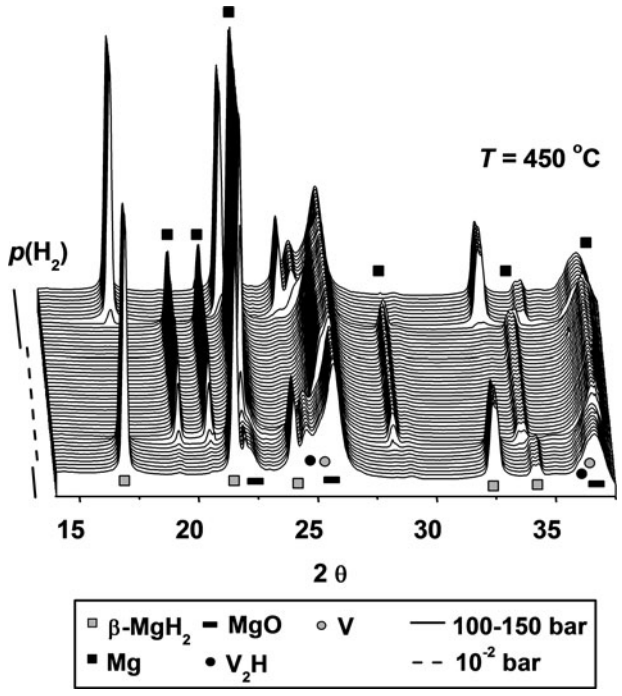

Figure 8. *In-situ* SR-PXD data of the activation process for sample MgH_2–V_2O_5 (S1) heated under $p(H_2) = 100$ bar from 320 to 450 °C (15 °C min^{-1}) and subsequently cycled at this temperature applying alternately $p(H_2) = 10^{-2}$ and 100–150 bar ($\lambda = 0.946\ 08$ Å).

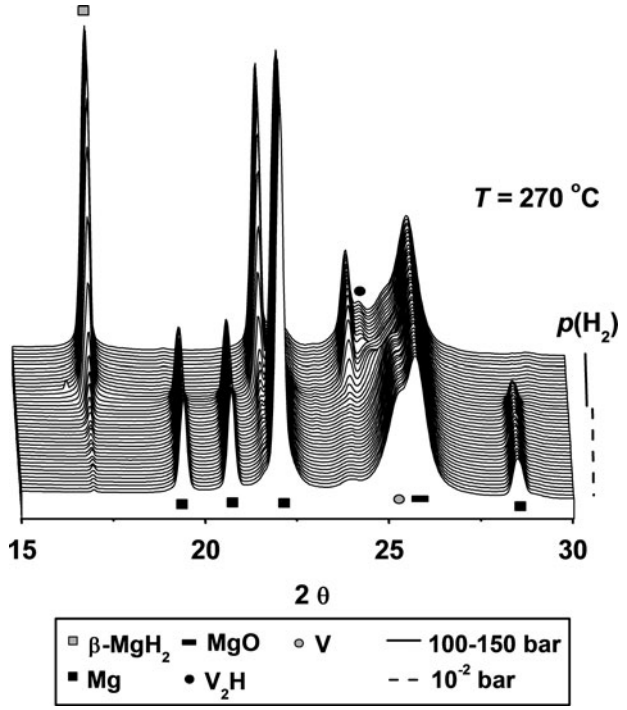

Figure 9. *In-situ* SR-PXD data of post-activation desorption measured for sample MgH_2–V_2O_5 (S1) cooled from 450 to 270 °C under $p(H_2) = 100$ bar (15 °C min^{-1}) where the pressure was decreased to $p(H_2) = 10^{-2}$ bar ($\lambda = 0.946\ 08$ Å).

The activation procedure, i.e., cycling at 450 °C clearly improves the desorption kinetics. This is illustrated in Figure 10 where extracted decomposition curves for MgH_2 are shown using data from Figures 1 and 9. After the activation process (Figure 8) the release of hydrogen from MgH_2 is both faster and more complete. This may be related to the formation of more V_2H/V in the sample and the fact that the hydrogen permeability of vanadium is large and exceeds that of palladium (Dolan, 2010). It is known that Nb and V based alloys are promising membranes materials, which currently are developed instead of Pd based alloys (Yukawa *et al.*, 2012). Therefore, the V_2H/V system may be the active catalytic component for the MgH_2–V_2O_5 system.

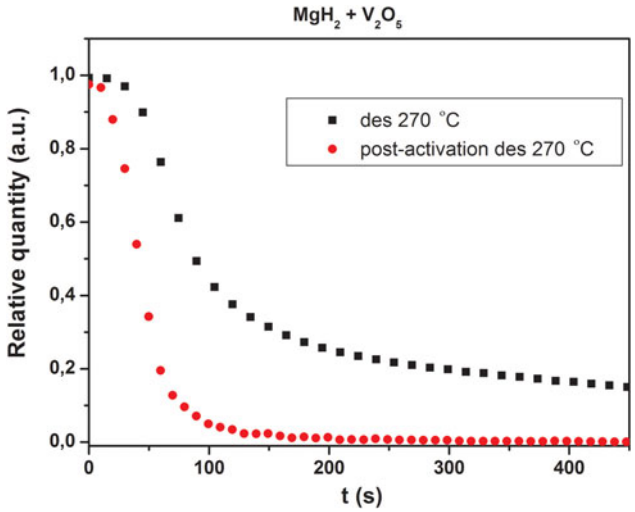

Figure 10. (color online) Comparison of the kinetic curves for MgH_2 decomposition at 270 °C before and after the activation of MgH_2–V_2O_5 (S1).

https://doi.org/10.1017/S0885715615000056 Published online by Cambridge University Press

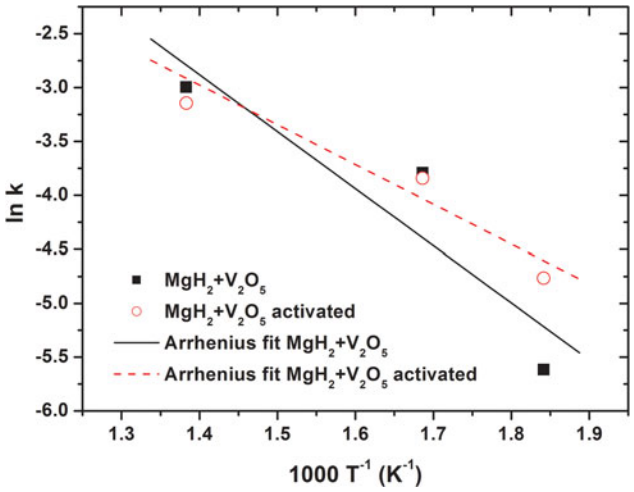

Figure 11. (color online) Arrhenius plot of the kinetic data for dehydrogenation of MgH_2–V_2O_5 (S1).

D. Apparent activation energy for the MgH_2 decomposition

The decomposition curves for MgH_2–V_2O_5 (S1) can be fitted well using the contracting surface model (two-dimensional growth) (Bamford and Tipper, 1980), e.g., kinetic shrinking core model, which suggests that hydrogen desorption is interface controlled (Liang *et al.*, 2000; Varin *et al.*, 2009).

An Arrhenius plot of the natural logarithm to the rate constant as a function of inverse temperature is provided in Figure 11. The calculated apparent activation energy E_A = 43 kJ mol^{-1} is obtained for the MgH_2–V_2O_5 sample S1 after milling. This value compares well to the activation energy for long range hydrogen diffusion in bulk Mg determined from experimental data to be E_A = 40.2 kJ mol^{-1} (Renner and Grabke, 1978). For the fully activated sample S1 the compounds V/V_2H are identified to be the active catalytic compounds, which facilitate hydrogen release. The *in situ* SR-PXD data also allow to extract an apparent activation energy for the activated sample, E_A = 34 kJ mol^{-1} (see Figure 11). These measured values are low, in particular when compared with that for bulk (unmilled) and air-exposed MgH_2, E_A = 300 kJ mol^{-1} (Jensen *et al.*, 2006). Apparent activation energies of E_A = 52 and 120 kJ mol^{-1} are measured for mechano-chemically treated MgH_2 with and without vanadium (5 mol%) as additive (Liang *et al.*, 1999b, 2000).

Thus, this kinetic analysis reveals that *in situ* synthesis of small particles of V/V_2H in the sample during cycling appears to have a stronger catalytic effect on hydrogen release and uptake in magnesium/magnesium hydride system. This may be because of a more uniform distribution of catalytic active particles compared with mechano-chemically prepared samples of MgH_2–V. There are inherent difficulties with obtaining uniform distribution of ductile metals in MgH_2 in contrast to brittle oxides that tend to form more homogenous distributed samples. The drawback is that considerable amounts of inert MgO are formed during reduction of V_2O_5 in the MgH_2–V_2O_5 system.

E. On the catalytic properties of vanadium pentoxide and vanadium metal

There are several studies that report high catalytic activity of V_2O_5 for release and uptake in magnesium hydride (Oelerich *et al.*, 2001a, 2001b; Barkhordarian *et al.*, 2006; Jung *et al.*, 2006). Vanadium(V) oxide, similar to niobium (V) oxide, is readily reduced in contact with hydrogen or mechano-chemically treated with MgH_2 (Jung *et al.*, 2006; Nielsen and Jensen, 2012). Several lower oxides may act as intermediates during the formation of MgO. The final product is shown here to be vanadium, which also participate in hydrogen release and uptake via V/V_2H system.

As mentioned above vanadium does not form alloy or intermetallic compounds with Mg (Schimmel *et al.*, 2005) thus it can act as a pure catalyst. MgH_2-5 mol%V composite desorbs hydrogen at 473 K (under vacuum) and re-absorbs hydrogen rapidly even at RT (Liang *et al.*, 1999b). The desorption rate was the highest for this mixture and decreased in the following order of additives: Ti, Mn, Fe, and Ni (Liang *et al.*, 1999a).

Moreover, MgH_2-5 mol%V system has the fastest kinetics for hydrogen release and uptake in magnesium hydride in comparison with Ti and is similar to Nb additive (Charbonnier *et al.*, 2004). Mg-10 wt.%V system exhibits the highest rate of hydrogen desorption and shows the lowest activation energy among Y and Zr additives (Czujko *et al.*, 2006). In addition, vanadium itself reversibly absorbs and desorbs 2.3 wt% of hydrogen at RT, which is also larger than that of the known alloys, $LaNi_5$, FeTi (Varin *et al.*, 2009; Nakamura *et al.*, 2012).

IV. CONCLUSION

Using the same conditions for the synthesis (mechano-chemical treatment) and evaluation of properties (hydrogen-vacuum cycling) a comparative analysis was carried out and the best from the studied catalysts for desorption/absorption of hydrogen for commercial powder MgH_2 was determined. It was found that the fastest kinetics at 320 °C shows the sample with additive of 5 mol% V_2O_5. Additional activation of the system (2 cycles at 450 °C) leads to the significant improvement and acceleration of kinetics even at lower 270 °C temperature. Observed effect is achieved through the full reduction of vanadium oxides, the formation of new efficient catalyst in the form of ultrafine particles of vanadium and purification of interface MgH_2/V in the process of heating to 450 °C in dynamic vacuum. This reduces the apparent activation energy of hydrogen desorption below the values of the activation energy of hydrogen diffusion in Mg, owing to the joint effect of nanostructuring and high hydrogen permeability of vanadium catalyst, which strongly bound to the surface of the MgH_2 crystallites. Thus the real catalyst for the hydrogen release/uptake in the MgH_2 is nanoparticles of pure vanadium obtained by the full reduction of V_2O_5 that was used originally.

ACKNOWLEDGEMENTS

The authors acknowledge funding for this research from the Danish Research Council for Natural Sciences (Danscatt). Moreover, the work was supported by the Danish National Research Foundation (Centre for Materials Crystallography), the Danish Strategic Research Council (Centre for Energy Materials), and the Carlsberg Foundation and the Swedish Research Council. The access to beam time at the MAX II synchrotron, Lund, Sweden in the research laboratory MAX-lab is gratefully acknowledged. Support from EU COST action MP1103 is also acknowledged.

https://doi.org/10.1017/S0885715615000056 Published online by Cambridge University Press

Andreasen, A., Sorensen, M. B., Burkarl, R., Moller, B., Molenbroek, A. M., Pedersen, A. S., Andreasen, J. W., Nielsen, M. M., and Jensen, T. R. (**2005**). "Interaction of hydrogen with an Mg-Al alloy," J. Alloys Compd. **404**, 323–326.

Andreasen, A., Sørensen, M. B., Burkarl, R., Møller, B., Molenbroek, A. M., Pedersen, A. S., Vegge, T., and Jensen, T. R. (**2006**). "Dehydrogenation kinetics of air-exposed MgH_2/Mg_2Cu and $MgH_2/MgCu_2$ studied with *in situ* X-ray powder diffraction," Appl. Phys. A Mater **82**, 515–521.

Bamford, C. H. and Tipper, C. F. H. (**1980**). "Theory of solid state reaction kinetics," in *Comprehensive Chemical Kinetics*, Brown, M. E., Dollimore, D., and Galwey, A. K., eds. (Elsevier, Amsterdam, Netherlands), Vol. 22, pp. 41–113.

Barkhordarian, G., Klassen, T., and Bormann, R. (**2006**). "Catalytic mechanism of transition-metal compounds on Mg hydrogen sorption reaction," J. Phys. Chem. B **110**, 11020–11024.

Bhat, V. V., Rougier, A., Aymard, L., Darok, X., Nazri, G., and Tarascon, J. M. (**2006**). "Catalytic activity of oxides and halides on hydrogen storage of MgH_2," J. Power Sources **159**, 107–110.

Callini, E., Pasquini, L., Rude, L. H., Nielsen, T. K., Jensen, T. R., and Bonetti, E. (**2010**). "Hydrogen storage and phase transformations in Mg-Pd nanoparticles," J. Appl. Phys. **108**, 073513.

Callini, E., Pasquini, L., Jensen, T. R., and Bonetti, E. (**2013**). "Hydrogen storage properties of Mg-Ni nanoparticles," Int. J. Hydrog. Energy **38**, 12207–12212.

Charbonnier, J., de Rango, P., Fruchart, D., Miraglia, S., Pontonnier, L., Rivoirard, S., Skryabina, N., and Vulliet, P. (**2004**). "Hydrogenation of transition element additives (Ti, V) during ball milling of magnesium hydride," J. Alloys Compd. **383**, 205–208.

Cuevas, F., Korablov, D., and Latroche, M. (**2012**). "Synthesis, structural and hydrogenation properties of Mg-rich MgH_2-TiH_2 nanocomposites prepared by reactive ball milling under hydrogen gas," Phys. Chem. Chem. Phys. **14**, 1200–1211.

Czujko, T., Varin, R. A., Chiu, C., and Wronski, Z. (**2006**). "Investigation of the hydrogen desorption properties of Mg + 10wt.%X (X = V, Y, Zr) submicrocrystalline composites," J. Alloys Compd. **414**, 240–247.

Deledda, S., Borissova, A., Poinsignon, C., Botta, W. J., Dornheim, M., and Klassen, T. (**2005**). "H-sorption in MgH_2 nanocomposites containing Fe or Ni with fluorine," J. Alloys Compd. **404–406**, 409–412.

Dolan, M. D. (**2010**). "Non-Pd BCC alloy membranes for industrial hydrogen separation," J. Membr. Sci. **362**, 12–28.

Hammersley, A. P., Svensson, S. O., Hanfland, M., Fitch, A. N., and Hausermann, D. (**1996**). "Two-dimensional detector software: from real detector to idealised image or two-theta scan," High Press. Res. **14**, 235–248.

Hirokazu, K. and Kitagawa, H. (**2012**). "Nanostructured materials for hydrogen storage," *Int. Symp. on Metal-Hydrogen Systems*, Kyoto, Japan, p. 187.

Huot, J., Liang, G., Boily, S., Van Neste, A., and Schulz, R. (**1999**). "Structural study and hydrogen sorption kinetics of ball-milled magnesium hydride," J. Alloys Compd. **293**, 495–500.

Huot, J., Ravnsbæk, D. B., Zhang, J., Cuevas, F., Latroche, M., and Jensen, T. R. (**2013**). "Mechanochemical synthesis of hydrogen storage materials," Progr. Mater. Sci. **58**, 30–75.

Ivanov, E., Konstanchuk, I., Bokhonov, B., and Boldyrev, V. (**2003**). "Hydrogen interaction with mechanically alloyed magnesium-salt composite materials," J. Alloys Compd. **359**, 320–325.

Jensen, T. R., Andreasen, A., Vegge, T., Andreasen, J. W., Stahl, K., Pedersen, A. S., Nielsen, M. M., Molenbroek, A. M., and Besenbacher, F. (**2006**). "Dehydrogenation kinetics of pure and nickel-doped magnesium hydride investigated by *in situ* time-resolved powder X-ray diffraction," Int. J. Hydrog. Energy **31**, 2052–2062.

Jensen, T. R., Nielsen, T. K., Filinchuk, Y., Jorgensen, J. E., Cerenius, Y., Gray, E. M., and Webb, C. J. (**2010**). "Versatile *in situ* powder X-ray diffraction cells for solid-gas investigations," J. Appl. Crystallogr. **43**, 1456–1463.

Jin, S.-A., Shim, J.-H., Ahn, J.-P., Cho, Y. W., and Yi, K.-W. (**2007a**). "Improvement in hydrogen sorption kinetics of MgH_2 with Nb hydride catalyst," Acta Mater. **55**, 5073–5079.

Jin, S. A., Shim, J. H., Cho, Y. W., and Yi, K. W. (**2007b**). "Dehydrogenation and hydrogenation characteristics of MgH_2 with transition metal fluorides," J. Power Sources **172**, 859–862.

Jung, K. S., Lee, E. Y., and Lee, K. S. (**2006**). "Catalytic effects of metal oxide on hydrogen absorption of magnesium metal hydride," J. Alloys Compd. **421**, 179–184.

Kim, J. W., Ahn, J. P., Jin, S. A., Lee, S. H., Chung, H. S., Shim, J. H., Cho, Y. W., and Oh, K. H. (**2008**). "Microstructural evolution of NbF_5-doped MgH_2 exhibiting fast hydrogen sorption kinetics," J. Power Sources **178**, 373–378.

Liang, G., Huot, J., Boily, S., Van Neste, A., and Schulz, R. (**1999a**). "Catalytic effect of transition metals on hydrogen sorption in nanocrystalline ball milled MgH_2–Tm (Tm = Ti, V, Mn, Fe and Ni) systems," J. Alloys Compd. **292**, 247–252.

Liang, G., Huot, J., Boily, S., Van Neste, A., and Schulz, R. (**1999b**). "Hydrogen storage properties of the mechanically milled MgH_2–V nanocomposite," J. Alloys Compd. **291**, 295–299.

Liang, G., Huot, J., Boily, S., and Schulz, R. (**2000**). "Hydrogen desorption kinetics of a mechanically milled MgH_2 + 5at.%V nanocomposite," J. Alloys Compd. **305**, 239–245.

Ma, L. P., Kang, X. D., Dai, H. B., Liang, Y., Fang, Z. Z., Wang, P. J., Wang, P., and Cheng, H. M. (**2009**). "Superior catalytic effect of TiF_3 over $TiCl_3$ in improving the hydrogen sorption kinetics of MgH_2: catalytic role of fluorine anion," Acta Mater. **57**, 2250–2258.

Malka, I. E., Czujko, T., and Bystrzycki, J. (**2010**). "Catalytic effect of halide additives ball milled with magnesium hydride," Int. J. Hydrog. Energy **35**, 1706–1712.

Massalski, T. B. (**1990**). *Binary Alloy Phase Diagrams* (ASM International, Materials Park, OH, USA).

Nakamura, J., Kato, N., Takamatsu, Y., Fuura, T., Oosawa, M., and Tsunokake, S. (**2012**). "Hydrogen storage properties of the Ti-V-Cr-Fe alloy used vanadium obtained by thermite reaction," *Int. Symp. on Metal-Hydrogen Systems*, Kyoto, Japan, p. 121.

Nielsen, T. K. and Jensen, T. R. (**2012**). "MgH_2-Nb_2O_5 investigated by *in situ* synchrotron X-ray diffraction," Int. J. Hydrog. Energy **37**, 13409–13416.

Nielsen, T. K., Manickam, K., Hirscher, M., Besenbacher, F., and Jensen, T. R. (**2009**). "Confinement of MgH_2 nanoclusters within nanoporous aerogel scaffold materials," ACS Nano **3**, 3521–3528.

Nielsen, T. K., Besenbacher, F., and Jensen, T. R. (**2011**). "Nanoconfined hydrides for energy storage," Nanoscale **3**, 2086–2098.

Oelerich, W., Klassen, T., and Bormann, R. (**2001a**). "Comparison of the catalytic effects of V, V_2O_5, VN, and VC on the hydrogen sorption of nanocrystalline Mg," J. Alloys Compd. **322**, L5–L9.

Oelerich, W., Klassen, T., and Bormann, R. (**2001b**). "Metal oxides as catalysts for improved hydrogen sorption in nanocrystalline Mg-based materials," J. Alloys Compd. **315**, 237–242.

Paskevicius, M., Sheppard, D. A., and Buckley, C. E. (**2010**). "Thermodynamic changes in mechanochemically synthesized magnesium hydride nanoparticles," J. Am. Chem. Soc. **132**, 5077–5083.

Pasquini, L., Callini, E., Brighi, M., Boscherini, F., Montone, A., Jensen, T. R., Maurizio, C., Antisari, M. V., and Bonetti, E. (**2011**). "Magnesium nanoparticles with transition metal decoration for hydrogen storage," J. Nanopart. Res. **13**, 5727–5737.

Renner, J. and Grabke, H. J. (**1978**). "Determination of diffusion coefficients in the hydriding of alloys," Mater. Res. Adv. Tech. **69**, 639–642.

Rodríguez-Carvajal, J. (**1993**). "Recent advances in magnetic structure determination by neutron powder diffraction," Physica B **192**, 55–69.

Sato, M. and Ishikawa, S. (**2012**). "Reversible multi step hydrogen absorption and desorption by $Mg_{12}Zn_{13}$," *Int. Symp. on Metal-Hydrogen Systems*, Kyoto, Japan, p. 100.

Schimmel, H. G., Huot, J., Chapon, L. C., Tichelaar, F. D., and Mulder, F. M. (**2005**). "Hydrogen cycling of niobium and vanadium catalyzed nanostructured magnesium," J. Am. Chem. Soc. **127**, 14348–14354.

Vajo, J. J. (**2011**). "Influence of nano-confinement on the thermodynamics and dehydrogenation kinetics of metal hydrides," Curr. Opin. Solid State Mater. Sci. **15**, 52–61.

Varin, R. A., Czujko, T. and Wronski, Z. S. (**2009**). *Nanomaterials for Solid State Hydrogen Storage* (Springer, New York).

Varin, R. A., Zbroniec, L., Polanski, M., and Bystrzycki, J. (**2011**). "A review of recent advances on the effects of microstructural refinement and nanocatalytic additives on the hydrogen storage properties of metal and complex hydrides," Energies **4**, 1–25.

Yukawa, H., Nambu, T., and Matsumoto, Y. (**2012**). "Hydrogen solubility and permeability of V-W-Mo alloy membrane for hydrogen separation and purification," *Int. Symp. on Metal-Hydrogen Systems*, Kyoto, Japan, p. 426.